TR-o-0037 48

Superresolution of Multipath Delay Profiles Measured by PN Correlation Method and Its Application to Indoor Propagation Analyses

Takeshi Manabe and Hitoshi Takai

March 31 1991

ATR Optical and Radio Communications Research Laboratories

Abstract

Time resolution of multipath delay profiles measured by using autocorrelation of pseudonoise (PN) code sequence is generally limited by the chip interval of the PN code sequence. In this paper, we propose a superresolution PN correlation method (SPM) which improves the time resolution of delay profiles measured by the conventional PN correlation method. The SPM is based on a decomposition of the eigenvector space of the correlation matrix delay-profile data vector and gives the number of paths and their delay times with higher resolution. It is verified by computer simulations and experiments using coaxial delay lines that the SPM can resolve two paths with a delay difference of a few tenths of the chip interval. Applicability of the SPM to the analysis of indoor multipath environment in which many delayed waves arrive with short delay differences is demonstrated by a indoor radio propagation experiment at 240 MHz, 910 MHz, and 2.3 GHz.

T. Manabe was with ATR Optical and Radio Communications Research Laboratories, Seika-cho, Soraku-gun, Kyoto 619-02, Japan. He is now with the Communications Research Laboratory, Koganei, Tokyo 184, Japan.

H. Takai was with ATR Optical and Radio Communications Research Laboratories, Seika-cho, Soraku-gun, Kyoto 619-02, Japan. He is now with Kansai Information and Communications Research Laboratory, Matsushita Electric Industrial Co., Ltd., Moriguchi, Osaka 570, Japan.

Contents

List of Figures

I. Introduction

In indoor digital radio communication systems, multipath propagation due to reflection of radiowaves by walls, office fixtures, or other furniture, can often lead to severe performance degradation giving rise to intersymbol interference which limits the signal transmission rate of the system. To analyze multipath propagation, delay profiles which correspond to the impulse responses of the transmission channel are widely used in land mobile communications[1]. In recent years, measurement of indoor delay profiles within office and factory buildings has become an active area of research[2]. Considering the scale of the environmental structures concerning indoor multipath propagation, the delay-time resolution required for indoor propagation analysis is much higher than that required for urban mobile propagation analysis.

Various methods have been employed to measure the indoor delay profiles, which are classified as follows: 1) to measure the impulse response directly by transmitting a short rf pulse[3][4][5]; 2) to measure the channel transfer function in the frequency domain by scanning an unmodulated carrier frequency[6][7]; 3) to infer the impulse response by correlation techniques by transmitting a pseudonoise (PN) code sequence[8][9][10]. We hereafter refer to the method classified into the category 3 as the *PN correlation method.* The PN correlation method, owing to the process gain in the correlation process, has the advantage over other methods due to its immunity from interference from other radio systems operating in the same frequency band. The required transmission power spectral density, therefore, can be much lower in the PN correlation method than in other methods. The drawback of the conventional PN correlation method is that the delay-time resolution is limited to the chip interval of the PN sequence. Although high-resolution delay profiles are necessary to analyze indoor radio propagation, almost all measurements of the indoor delay profiles reported so far have been made using PN sequences with chip rates of several

tens of MHz, and the resultant resolution of the path difference is not less than several meters, which is not sufficient to analyze the indoor multipath propagation in detail.

As for the method 1), there have been a few studies on application of the MUSIC method [11] to improve the delay-time resolution [12][13]. On the other hand, 3). no approach has been made to improve the resolution of delay profiles measured by the method

In this paper, we propose a superresolution method to improve the time resolution of delay profiles measured by the conventional PN correlation method[14][15]. We refer to this method as the superresolution PN correlation method (SPM) throughout this paper. The SPM algorithm is based on the eigen-decomposition of the correlation matrix for the delay-profile data vector similar to the MUSIC algorithm used in spectrum analyses such as the direction-of-arrival (DOA) estimation by an array of antennas [11]. In Section II, we formulate the delay-profile estimation problem based on the conventional PN correlation method. In Sections III and IV, we propose the SPM to improve the delay-time resolution. In Section V, we introduce a method to estimate the complex impulse response of the multipath transmission channel from the delay times estimated by the SPM. Results of computer simulations and experiments are presented in Sections VI and VII, respectively.

II. Delay Profiles Measured by Conventional PN Correlation Method

If an rf signal $u(t)$ is transmitted over a multipath transmission channel, the received rf signal $y(t)$ is expressed in terms of the convolution of the transmitted signal and the impulse response $h(t)$ of the channel as

$$y(t) = \int_{-\infty}^{\infty} h(\tau)u(t-\tau)d\tau. \tag{II.1}$$

Consider a case in which the multipath transmission channel consists of M discrete paths with different delay times. With this discrete channel model, its impulse response can be expressed as

$$h(t) = \sum_{i=1}^{M} h_i \delta(t - T_i), \tag{II.2}$$

where T_i is the propagation delay of the ith path, and $\delta(\cdot)$ is the Dirac delta function. For a transmitted signal given by $\mathrm{Re}[x(t)e^{j\omega t}]$, where $x(t)$ is the baseband modulation signal and ω is the carrier angular frequency, the received signal is expressed in the equivalent low-pass system as

$$v(t) = \sum_{i=1}^{M} h_i x(t - T_i) e^{-j\omega T_i} + \nu(t), \tag{II.3}$$

where $\nu(t)$ is the equivalent low-pass additive white noise at the receiver input. The additive noise $\nu(t)$ is assumed to be a zero-mean stationary random process independent of the transmitted signal.

In the conventional PN correlation method, a pseudonoise (PN) code sequence is employed as the baseband modulation signal $x(t)$ to modulate the transmitted carrier. At the receiving end, the received signal is correlated with the replica of the transmitted PN code sequence. Then, the correlator output yields an estimate of the delay profile of the transmission channel between the transmitter and receiver due to the fact that the autocorrelation function of the PN sequence can be approximately given by the delta function. If the correlation is taken over a time interval T, the complex-valued delay profile measured by this method is given by

$$z(\tau) = \frac{1}{T} \int_0^T x(t - \tau) v(t) dt, \tag{II.4}$$

and $|z(\tau)|^2$ is referred to as the power delay profile. Substituting (II.3) into (II.4), the delay profile can be expressed as

$$z(\tau) = \sum_{i=1}^{M} h_i e^{-j\omega T_i} r(\tau - T_i) + n(\tau). \tag{II.5}$$

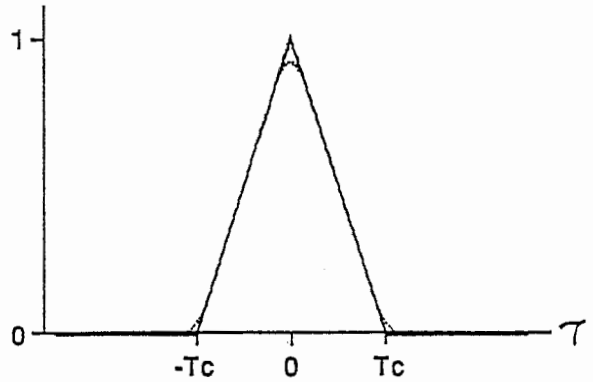

Figure II.1. Autocorrelation functions of m-sequence generated by a 10-stage shift register without band-limitation (solid line) and with band-limitation of $BT_c = 1.325$ ($\sigma = 0.1\ T_c$).

In (II.5), $r(\tau)$ is the autocorrelation function of the transmitted PN sequence signal given by

$$r(\tau) = \frac{1}{T}\int_0^T x(t-\tau)x(t)dt, \tag{II.6}$$

and $n(\tau)$ is additive noise term given by

$$n(\tau) = \frac{1}{T}\int_0^T x(t-\tau)\nu(t)dt. \tag{II.7}$$

In measuring the delay profiles, a maximal-length shift-register sequence (m-sequence) is commonly used as a PN sequence. However the autocorrelation function of m-sequence is not exactly the delta function with an infinitely narrow width but a triangular function with a spread of $\pm T_c$ around the correlation peak where T_c is the chip interval of the sequence as depicted by a solid line in Fig. II.1.[1] Due to this spread of the triangular autocorrelation function, the conventional PN correlation method can not resolve the

[1]In addition to the triangular peak, the autocorrelation function of m-sequence has a very small negative baseline offset. In the case of the 10-stage m-sequence, the baseline offset is -60 dB with respect to the main peak, which is too low to be appreciable in Fig. II.1.

Table II.1: Multipath transmission channel model used in Simulation I

Path	Delay Time	SN Ratio	Relative Phase
#1	1.2 T_c	40 dB	0°
#2	1.7 T_c	33 dB	180°
#3	3.6 T_c	20 dB	0°

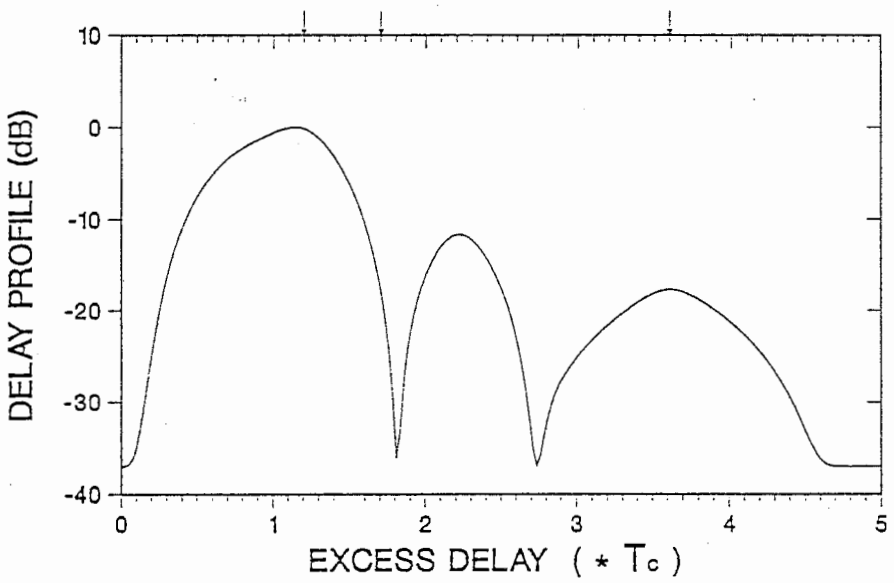

Figure II.2. Power delay profile of the transmission channel given in Table I by using the 10-stage m-sequence of chip rate T_c. Actual delay times of three paths are identified by small arrows.

delay times of multipath components arriving within an interval smaller than the chip interval T_c as is illustrated by a typical example given below.

Fig. II.2 shows the power delay profile calculated for a multipath model which consists of three discrete paths, the first two of which arrive with a delay difference of 0.5 T_c, and the third of which differs from the second by 1.9 T_c. The relative delays, the signal-to-noise ratios, and the relative phases of the three paths are given in Table II.1. Here we

defined the signal-to-noise ratio of the ith path as $|h_i|^2/\sigma_n^2$ where σ_n^2 is the variance of $n(\tau)$. The actual delay times of the three paths are indicated by small arrows in Fig. II.2. It is found that the peaks due to the first two paths overlap each other and that these two overlapping paths form not only a sharp depression around the delay time of the second path but also a spurious peak around $2.2T_c$ by destructive and constructive interferences of the first two paths, respectively. This example demonstrates that power delay profiles measured by the conventional PN correlation method with insufficient resolution may be delusive in some cases and that they cannot be used for detailed analyses of indoor multipath environments.

Various measurements using the conventional PN correlation method have been reported for indoor multipath propagation. However, almost all of these measurements have been made using PN sequences with chip rates of several tens of MHz and the resultant resolution of the path difference is not less than several meters which is not sufficient to analyze the indoor multipath propagation in detail. Conceptually, the simplest method of improving the time delay resolution of the PN correlation method is to increase the chip rate of the PN sequence. However, this requires hardware complexity in the transmitters and receivers. The higher the chip rate of the PN sequence, the more difficult and the more complex it becomes to implement the digital circuitry. In what follows, we propose another method, the superresolution PN correlation method (SPM), to improve the resolution of the delay profile measured by the conventional PN correlation method without any changes in the hardware.

III. Superresolution Estimation of Multipath Delay Times

Prepare a delay-profile data vector $\boldsymbol{z}$ by sampling the delay profile $z(\tau)$ obtained as a function of relative delay τ at the output of the correlator at K discrete delay times $\{\tau_1, \tau_2, \cdots, \tau_K\}$ such that $\boldsymbol{z} = (z(\tau_1), z(\tau_2), \cdots, z(\tau_K))^t$. In what follows, we assumed that the sampling interval is chosen to be a small fraction of the chip interval T_c of the PN sequence. From (II.5), the data vector $\boldsymbol{z}$ is expressed as

$$\boldsymbol{z} = \sum_{i=1}^{M} h_i e^{-j\omega T_i} \boldsymbol{r}(T_i) + \boldsymbol{n}. \tag{III.1}$$

In (III.1), $\boldsymbol{r}(T_i)$ is the mode vector defined as $\boldsymbol{r}(T_i) = (r(\tau_1 - T_i), r(\tau_2 - T_i), \cdots, r(\tau_K - T_i))^t$, and $\boldsymbol{n} = (n(\tau_1), n(\tau_2), \cdots, n(\tau_K))^t$, where ^{t} denotes transpose. The correlation matrix $\boldsymbol{R}$ of this data vector $\boldsymbol{z}$ is expressed as

$$\begin{aligned} \boldsymbol{R} &= E[\boldsymbol{z}\boldsymbol{z}^\dagger] \\ &= \sum_{i,j} h_i h_j^* e^{j\omega(T_j - T_i)} \boldsymbol{r}(T_i) \boldsymbol{r}(T_j)^t + E[\boldsymbol{n}\boldsymbol{n}^\dagger], \end{aligned} \tag{III.2}$$

where † and * denote Hermitian and complex conjugates, respectively, and $E[\cdot]$ denotes the expected value. Substituting (II.7) into the second term in the right-hand side of (III.2), the noise correlation matrix $E[\boldsymbol{n}\boldsymbol{n}^\dagger]$ can be expressed as

$$E[\boldsymbol{n}\boldsymbol{n}^\dagger] = \sigma_n^2 \boldsymbol{R}_0 \tag{III.3}$$

where $\boldsymbol{R}_0$ is a symmetric matrix whose klth element is $r(\tau_k - \tau_l)$. It should be noted that the additive noise $n(\tau)$ given by (II.7) is not white but colored, with a finite correlation time T_c, even though $\nu(\tau)$ is white noise, and $\boldsymbol{R}_0$, therefore, is not the identity matrix because the sampling interval is a small fraction of T_c.

As in the MUSIC algorithm used for DOA estimation[11], the SPM to be proposed here is based on decomposition of the eigenvector space of the correlation matrix $\boldsymbol{R}$ into signal

subspace and noise subspace, and the number of paths is determined by the dimension of the signal subspace. In multipath delay time estimation, however, the dimension of the signal subspace, i.e. the rank of the signal correlation matrix $\boldsymbol{R}-\sigma_n^2\boldsymbol{R}_0$, always reduces to unity due to the degeneracy of the signal subspace resulting from the inherent coherence among signals arriving via different paths. Accordingly, the number of paths cannot be determined directly form the eigen-decomposition of $\boldsymbol{R}$. This situation is the same as that encountered in DOA estimations by the MUSIC algorithm when the incident waves are mutually coherent [16]. In order for the SPM algorithm based on the eigen-decomposition to be applicable to this situation, the degeneracy of the signal subspace should be removed by decorrelating the mutual coherence of the multipath component signals.

The mutual coherence among different paths can be suppressed by averaging the correlation matrix over a range of carrier frequencies. This averaging can be accomplished by scanning the carrier frequency over $[\omega_0 - \frac{\Delta\omega}{2}, \omega_0 + \frac{\Delta\omega}{2}]$ around the center frequency ω_0, and the resultant correlation matrix $\bar{\boldsymbol{R}}$ becomes

$$\bar{\boldsymbol{R}} = \sum_{ij} h_i h_j^* e^{j\omega_0(T_j-T_i)} \frac{\sin\{\frac{\Delta\omega}{2}(T_j-T_i)\}}{\frac{\Delta\omega}{2}(T_j-T_i)} \boldsymbol{r}(T_i)\boldsymbol{r}(T_j)^t + \sigma_n^2\boldsymbol{R}_0 \qquad \text{(III.4)}$$

in which the mutual coherence is decorrelated according to the sinc function $\sin x/x$ as x increases. In actual measurements, the frequency averaging may be achieved by averaging the delay profile $\boldsymbol{z}(\omega_l)$ sampled at discrete frequencies ω_l $(l = 1, 2, \cdots, L)$ as

$$\bar{\boldsymbol{R}} = \frac{1}{L}\sum_{l=1}^{L} \boldsymbol{z}(\omega_l)\boldsymbol{z}(\omega_l)^\dagger. \qquad \text{(III.5)}$$

As a result of the decorrealtion, the rank of the averaged signal correlation matrix $(\bar{\boldsymbol{R}} - \sigma_n^2\boldsymbol{R}_0)$ becomes M. Then, the number of paths and the time delay can be estimated by an eigenvalue analysis as in the MUSIC method. Since $\boldsymbol{R}_0$ is not the identity matrix, the eigenvalue problem to be solved is given by a general eigenvalue equation as

$$\bar{\boldsymbol{R}}\, e_i = \lambda_i \boldsymbol{R}_0\, e_i, \quad i = 1, 2, \cdots, K. \qquad \text{(III.6)}$$

The number of discrete paths can be estimated by comparing the magnitude of the K generalized eigenvalues of (III.6), i.e., if the signal to noise ratio is sufficiently high, the M largest generalized eigenvalues are much larger than σ_n^2, while the remaining $K-M$ eigenvalues are comparable to σ_n^2. A computationally stable and efficient method to solve this type of generalized eigenvalue problem is introduced in Appendix A. The eigenvectors corresponding to the the $K-M$ smallest eigenvalues span the noise subspace which is orthogonal to the signal subspace spanned by those corresponding to the M largest eigenvalues. Once the number of paths has been estimated, a superresolution delay profile $S(\tau)$ can be estimated by

$$S(\tau) = \frac{r(\tau)^t R_0^{-1} r(\tau)}{\sum_{i=1}^{K-M} |r(\tau)^t e_i|^2}, \tag{III.7}$$

where $r(\tau)$ is the mode vector for delay time τ given by $r(\tau) = (r(\tau_1 - \tau), r(\tau_2 - \tau), \cdots, r(\tau_K - \tau))^t$ [17]. If the signal-to-noise ratio is sufficiently high, $S(\tau)$ has M sharp peaks which correspond to the delay time of the M discrete paths. Then the delay times can be determined from the peak positions of $S(\tau)$.

Although the SPM algorithm proposed here looks like the MUSIC algorithm in its formulation, what it does is quite different. In the MUSIC algorithm, the mode vector is formed by kernels of the Fourier transformation, and then the algorithm, when applied to time-domain data, estimates frequency domain spectra. On the other hand, in the SPM algorithm, the mode vector $r(\tau)$ is formed by triangular autocorrelation function with finite spread, and the algorithm estimates high-resolution time-domain spectra from time domain data.

IV. Effects of Finite Bandwidth

Thus far, we have ignored the effects of band-limitation in transmitter and receiver. In this case, it can be shown that, when the delay times of two or more paths fall within a sampling interval $\Delta\tau$ between adjacent sampling times of $z(\tau)$, they cannot be resolved, since the delay times can not be uniquely determined and then the solutions are indefinite (see Appendix B). As described in Appendix B, this is caused by the rectilinear waveform of the triangular autocorrelation function of the band-unlimited m-sequence.

However, in practice, transmitters and receivers are never free from band-limitation. If one takes the finite bandwidth of the experimental system into account, the autocorrelation function of the m-sequence is no longer triangular, but becomes blunted. Hence, we can get rid of the indefiniteness of the solution, and the paths arriving within a sampling interval $\Delta\tau$ can be resolved as shown below.

The basic configuration of the delay-profile measurement system and its approximate equivalent low-pass system are shown in Figs. IV.1(a) and IV.1(b), respectively. In Fig. IV.1(a), $h_T(t)$ represents the impulse response of all filtering in the transmitter, and $h_R(t)$ represents the impulse response of all filtering in the receiver. In the equivalent low-pass representation given in Fig. IV.1(b), all the filtering in the transmitter and the receiver is approximately represented by an impulse response $h_{TR}(t)$.

The effects of band-limitation can be taken into account in the SPM proposed in Section III just by replacing the autocorrelation function $r(\tau)$ with the band-limited autocorrelation function given by

$$\begin{aligned} \tilde{r}(\tau) &= \frac{1}{T}\int_0^T x(t-\tau)[h_{TR}(t) \otimes x(t)]dt \\ &= h_{TR}(\tau) \otimes r(\tau), \end{aligned} \tag{IV.1}$$

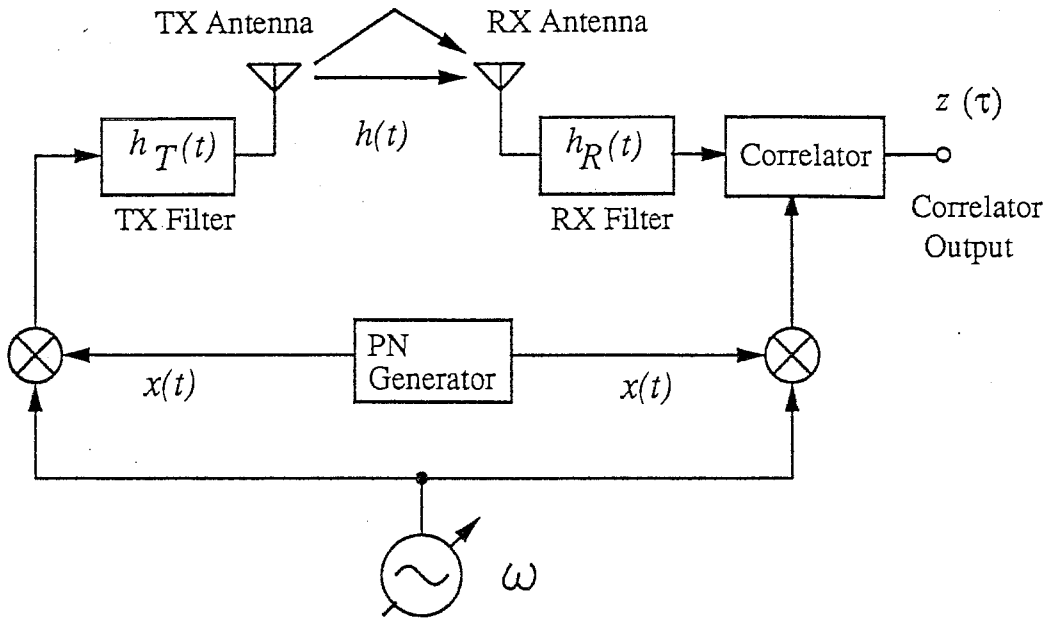

(a) Block diagram of the delay-profile measurement system

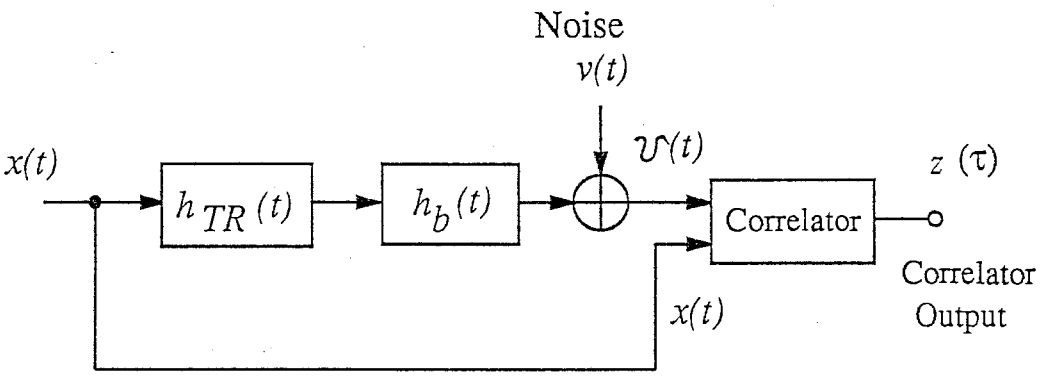

(b) its approximated equivalent low-pass representation (b). $h_b(t)$ is the equivalent low-pass channel impulse response. $[h_b(t) = \sum_{i=1}^{M} h_i e^{-j\omega T_i} \delta(t - T_i)$.

Figure IV.1: Basic configuration of the delay profile measurement system

where $\otimes$ denotes convolution.

In computer simulations and the analyses of experimental results described below, the effects of band-limitation are taken into account by assuming a Gaussian filter whose impulse response is given by

$$h_{TR}(\tau) = \frac{1}{\sqrt{2\pi}\,\sigma} e^{-\frac{\tau^2}{2\sigma^2}} \tag{IV.2}$$

where σ is a parameter characterizing the spread of the impulse response. The spread σ of this Gaussian impulse response is related to its 3-dB bandwidth B by $\sigma = \sqrt{\ln 2}/2\pi B$. The band-limited autocorrelation function of the m-sequence generated by a 10-stage shift register is shown by dotted curve in Fig. II.1 for band-limitation of $BT_c = 1.325$ ($\sigma = 0.1$ T_c).

V. Estimation of Complex Impulse Response

Although the peak positions of $S(\tau)$ give the delay times of multipath components, its peak magnitudes are not necessarily the measure of the relative amplitudes of the multipath components. However, as long as the multipath delay times are estimated with sufficient accuracy, the complex impulse response of the channel can be estimated by using the estimated delay times as follows.

By using the estimated delay times $\hat{T}_i$ ($i = 1, \cdots, M$), the delay profile measured at frequency ω_l can be expressed as

$$z(\omega_l) = \sum_{i=1}^{M} h_i e^{-j\omega_l \hat{T}_i} r(\hat{T}_i) + n, \qquad l = 1, 2, \cdots, L. \tag{V.1}$$

Here, we define the $KL\times 1$ vector z' by combining L data vectors as $z' = (z(\omega_1)^t, z(\omega_2)^t, \cdots, z(\omega_L)^t)^t$, and the impulse response vector as $h = (h_1, h_2, \cdots, h_M)^t$. The $KL\times 1$ vector z' is expressed as

$$z' = Ah + n', \tag{V.2}$$

where the $KL \times M$ matrix $\boldsymbol{A}$ is given by using the estimated delay times $\hat{T}_i$ ($i = 1, 2, \cdots, M$) as

$$\boldsymbol{A} = \begin{pmatrix} e^{-j\omega_1 \hat{T}_1} \hat{\boldsymbol{r}}_1 & e^{-j\omega_1 \hat{T}_2} \hat{\boldsymbol{r}}_2 & \cdots & e^{-j\omega_1 \hat{T}_M} \hat{\boldsymbol{r}}_M \\ e^{-j\omega_2 \hat{T}_1} \hat{\boldsymbol{r}}_1 & e^{-j\omega_2 \hat{T}_2} \hat{\boldsymbol{r}}_2 & \cdots & e^{-j\omega_2 \hat{T}_M} \hat{\boldsymbol{r}}_M \\ & \cdots & \cdots & \\ e^{-j\omega_L \hat{T}_1} \hat{\boldsymbol{r}}_1 & e^{-j\omega_L \hat{T}_2} \hat{\boldsymbol{r}}_2 & \cdots & e^{-j\omega_L \hat{T}_M} \hat{\boldsymbol{r}}_M \end{pmatrix}, \tag{V.3}$$

where $\hat{\boldsymbol{r}}_i$ is the $K \times 1$ column vector defined as $\hat{\boldsymbol{r}}_i = \boldsymbol{r}(\hat{T}_i)$.

By applying the least-squares method, an estimate of $\boldsymbol{h}$ is given by

$$\hat{\boldsymbol{h}} = (\boldsymbol{A}^\dagger \boldsymbol{R}_0'^{-1} \boldsymbol{A})^{-1} \boldsymbol{A}^\dagger \boldsymbol{R}_0'^{-1} \bar{\boldsymbol{z}}', \tag{V.4}$$

where $\bar{\boldsymbol{z}}'$ is the average of the observed data vector $\boldsymbol{z}'$ taken by repetitive frequency scanning, and $\boldsymbol{R}_0'$ is the $KL \times KL$ matrix defined as

$$\boldsymbol{R}_0' = \begin{pmatrix} \boldsymbol{R}_0 & 0 & 0 & \cdots & 0 \\ 0 & \boldsymbol{R}_0 & 0 & \cdots & 0 \\ 0 & 0 & \boldsymbol{R}_0 & \cdots & 0 \\ & \cdots & & \ddots & \\ 0 & 0 & 0 & \cdots & \boldsymbol{R}_0 \end{pmatrix}. \tag{V.5}$$

The ith component of $\hat{\boldsymbol{h}}$ gives an estimate $\hat{h}_i$ of the complex amplitude of the ith path and the estimated impulse response is given by $\hat{h}(t) = \sum_{i=1}^{M} \hat{h}_i \delta(t - \hat{T}_i)$.

VI. Computer Simulations

Computer simulations were carried out to demonstrate the performance of the SPM. In the following computer simulations, a 10-stage m-sequence was employed as a PN code sequence. After transmission through a discrete multipath channel model given by (II.2), the received signal was assumed to be corrupted by additive white noise modeled by a stationary complex-valued Gaussian process of zero mean.

VI.1. Simulation I

The SPM algorithm was applied to the delay profiles measured for the multipath transmission channel model given in Table II.1. As described in Section II, the first two paths cannot be resolved by the conventional PN correlation method. To apply the SPM algorithm, delay profiles were obtained at 11 different carrier frequencies ($L = 11$)

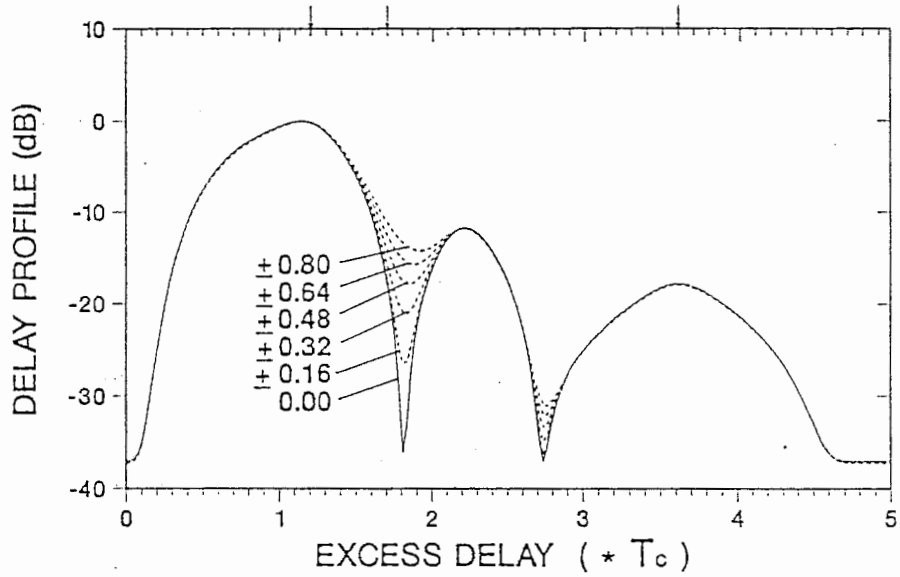

Figure VI.1. Power delay profile representation of the delay profile data used in Simulation I simulated for three-path transmission channel given in Table I. Parameters attached to curves are the carrier angular frequency deviation from center frequency in unit of T_c^{-1}

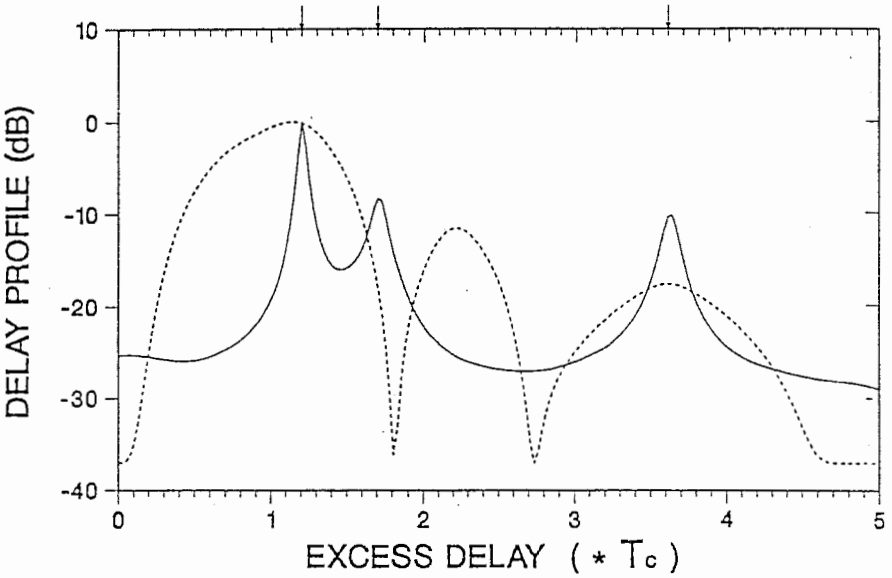

Figure VI.2. Superresolution delay profile estimated by the SPM (solid curve) for three-path transmission channel given in Table I. The dotted curve is the delay profile measured using the conventional PN correlation method at carrier center frequency ω_0.

equispaced in an angular-frequency interval of $[\omega_0 - 0.8 \times T_c^{-1},\ \omega_0 + 0.8 \times T_c^{-1}]$ around the carrier center frequency ω_0. Each delay profile was sampled with a sampling interval of $\Delta\tau = 0.2T_c$ over a delay-time interval from 0 to $5T_c$. Fig. VI.1 shows the power delay profiles at 11 different carrier frequencies used in this simulation[2]. Thus obtained data vectors $\boldsymbol{z}$ were used to form the correlation matrix as defined by (III.5). The SPM was applied to the correlation matrix $\tilde{\boldsymbol{R}}$ obtained by further averaging the thus obtained correlation matrix over 10 frequency scans. In this simulation, band-limitation modeled by a Gaussian filter given by (IV.2) with $BT_c = 1.325$ ($\sigma = 0.1\ T_c$) was assumed.

The result of applying the SPM is shown by a solid curve in Fig. VI.2 along with the power delay profile shown by a dotted curve obtained at the carrier center frequency ω_0

[2]Only five profiles can be identified in Fig. VI.1 because power delay profiles for positive and negative carrier-frequency deviations from ω_0 by the same amount differ only in noise which cannot be appreciable in Fig. VI.1 in this case.

by the conventional PN correlation method. It is found that three peaks appear in the estimated superresolution delay profile at correct positions corresponding to the actual delay times of the three paths. It is worthwhile noting that the peak corresponding to the second path, which cannot be identified in any of the 11 delay-profile data used in the estimation as shown in Fig. VI.1, is clearly identified at the correct position.

VI.2. Simulation II

In order to examine the delay-time resolution of two paths with small delay differences, computer simulations were carried out for a multipath transmission channel model which consisted of two paths with equal amplitudes and equal relative arrival phases. In this simulation, for the sake of comparison with experiments described below, the delay profiles were obtained at 5 equispaced frequencies over an angular-frequency interval of $[\omega_0 - 4.19 \times T_c^{-1},\ \omega_0 + 4.19 \times T_c^{-1}]$ around the carrier center frequency ω_0 and band-limitation of $BT_c = 0.7$ ($\sigma = 0.19\ T_c$) was assumed. Each delay profile was sampled with a sampling interval $\Delta\tau = 0.2\ T_c$ over a delay time interval from 0 to 4 T_c.

Solid curves in Fig. VI.3 show the results of estimation for delay differences of (a) 0.5 T_c, (b) 0.3 T_c, (c) 0.2 T_c, and (d) 0.15 T_c when that the signal-to-noise ratio of each path is 30 dB. Figs VI.4 and VI.5 show the similar results for signal-to-noise ratios of 35 and 40 dB, respectively. In these Figures, the delay profiles obtained by the conventional PN correlation method at the carrier center frequency ω_0 are also shown for comparison by dotted curves. When the delay-time difference is larger than 0.3 T_c, two paths are found to be clearly resolved by the SPM with sharp peaks pointing at the correct delay times. For signal-to-noise ratios above 35 dB, it is found that two paths can be resolved even when the delay-time difference is as small as 0.2 T_c.

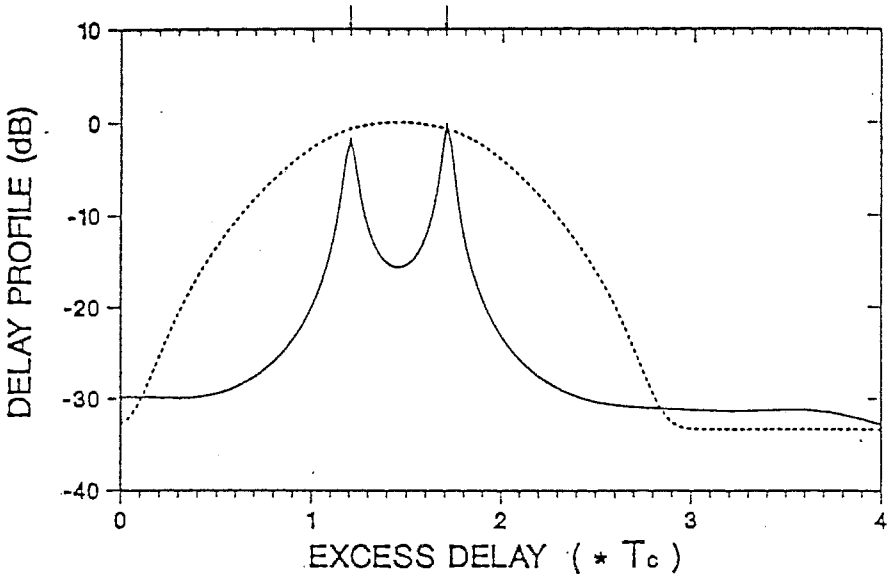

(a) Delay difference 0.5 T_c ($T_1 = 1.2T_c$, $T_2 = 1.7T_c$).

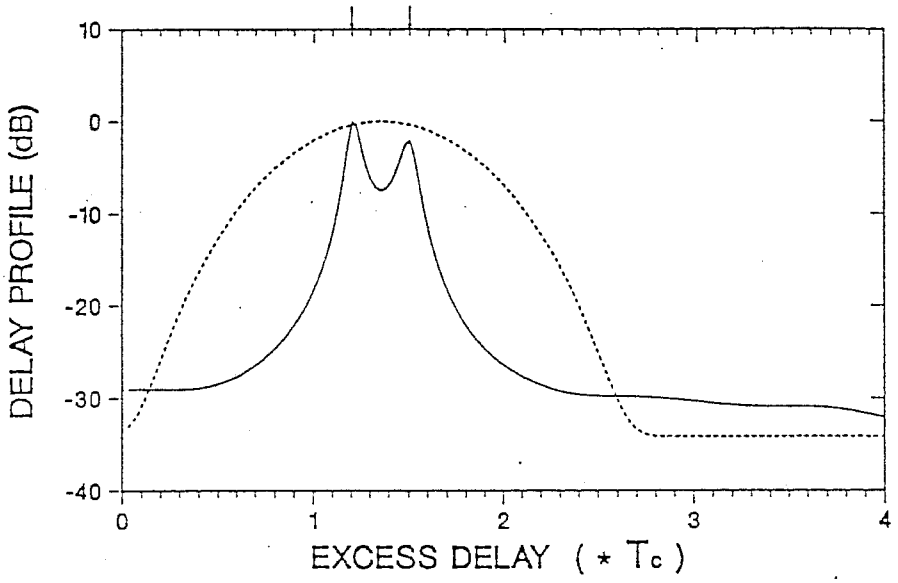

(b) Delay difference 0.3 T_c ($T_1 = 1.2T_c$, $T_2 = 1.5T_c$).

Figure VI.3. Superresolution delay profile estimated by the SPM for two-path transmission channels for delay differences of (a) 0.5 T_c, (b) 0.3 T_c, (c) 0.2 T_c, and (d) 0.15 T_c. Signal-to-noise ratios of the two paths are 30 dB and the band-limitation of $BT_c = 1.325$ ($\sigma = 0.1\ T_c$) is assumed.

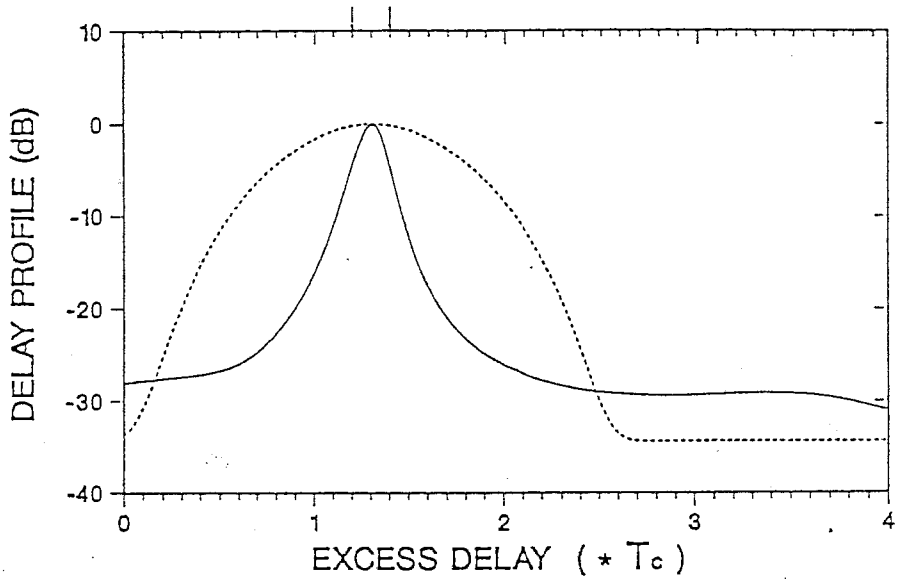

(c) Delay difference 0.2 T_c ($T_1 = 1.2T_c$, $T_2 = 1.4T_c$).

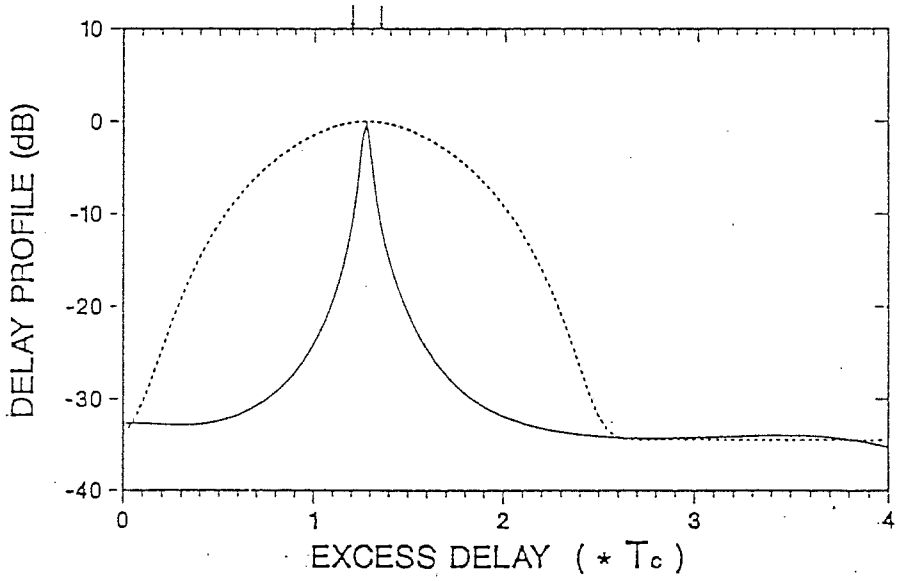

(d) Delay difference 0.15 T_c ($T_1 = 1.2T_c$, $T_2 = 1.35T_c$).

Figure VI.3: Contd.

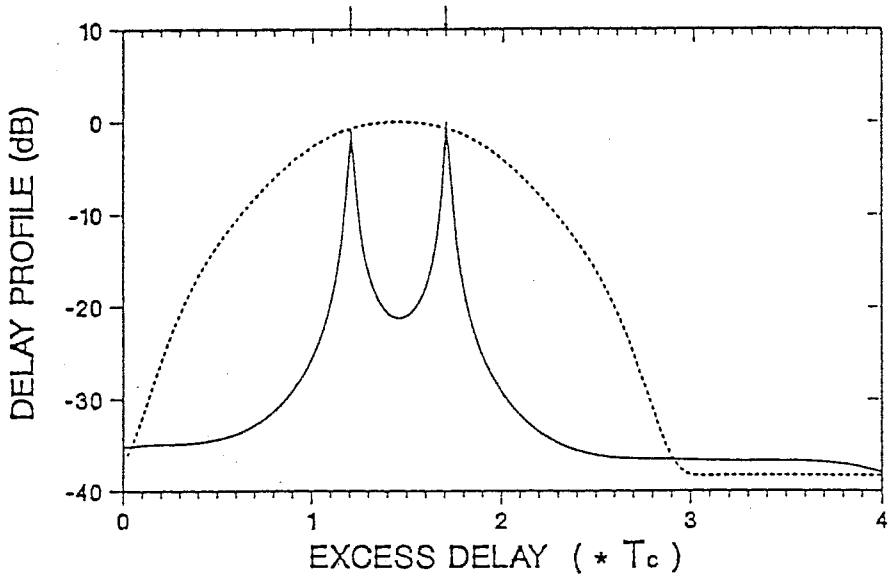

(a) Delay difference 0.5 T_c ($T_1 = 1.2T_c$, $T_2 = 1.7T_c$).

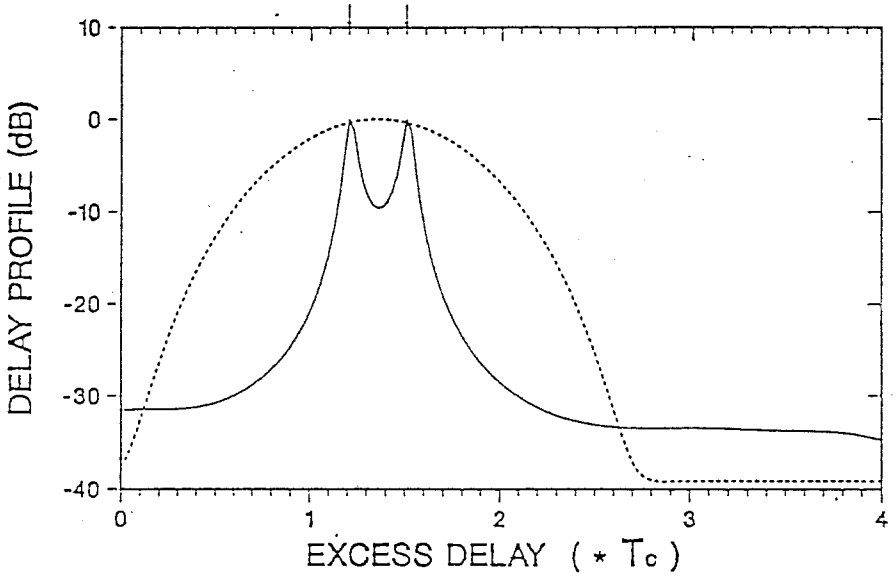

(b) Delay difference 0.3 T_c ($T_1 = 1.2T_c$, $T_2 = 1.5T_c$).

Figure VI.4: Same as Fig. VI.3 except that signal-to-noise ratios are 35 dB.

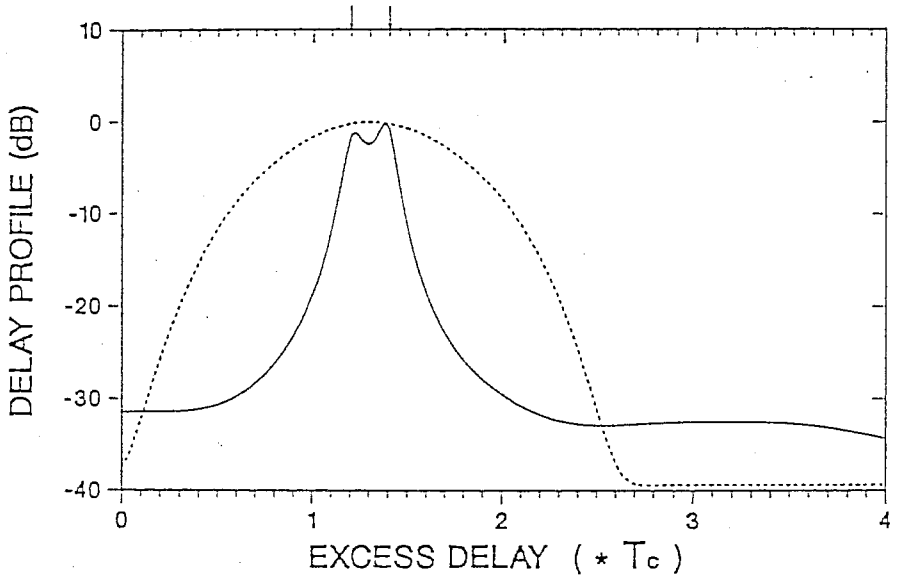

(c) Delay difference 0.2 T_c ($T_1 = 1.2T_c$, $T_2 = 1.4T_c$).

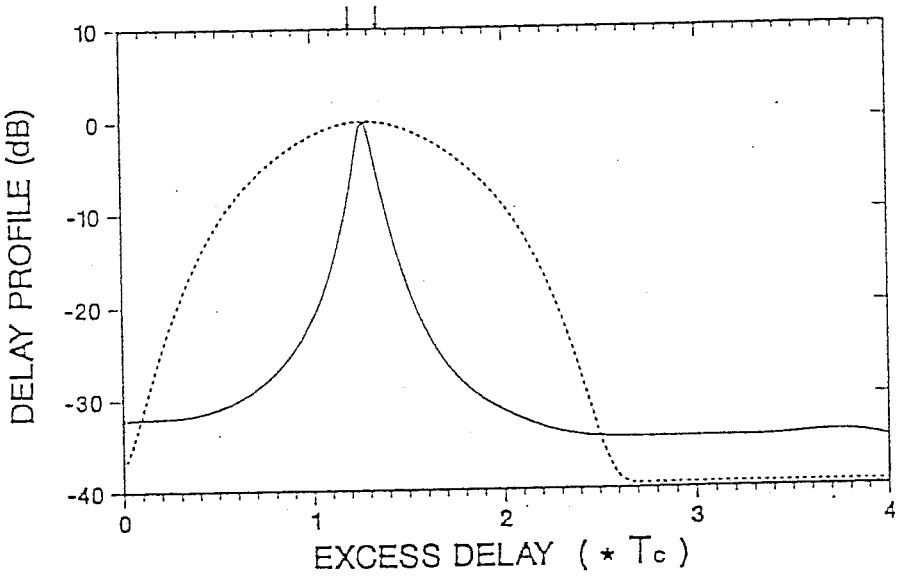

(d) Delay difference 0.15 T_c ($T_1 = 1.2T_c$, $T_2 = 1.35T_c$).

Figure VI.4: Contd.

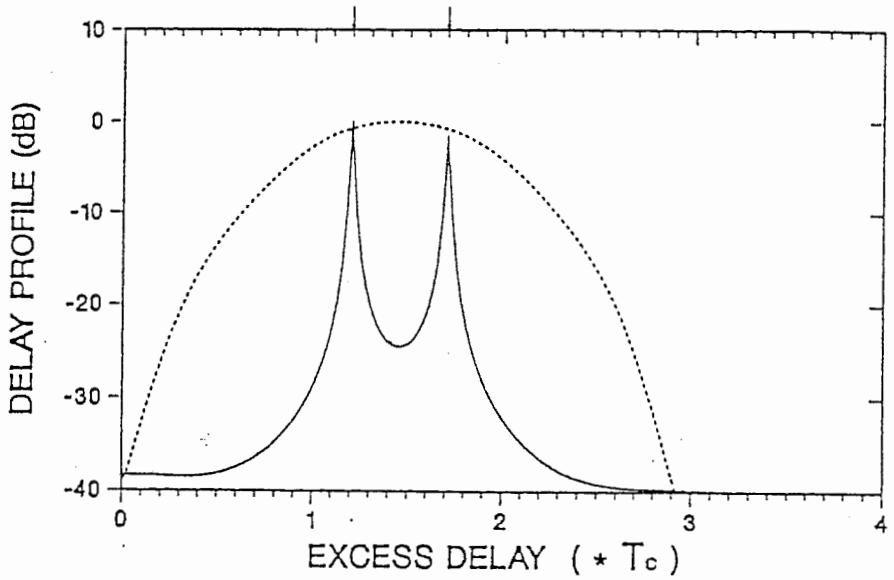

(a) Delay difference 0.5 T_c ($T_1 = 1.2T_c$, $T_2 = 1.7T_c$).

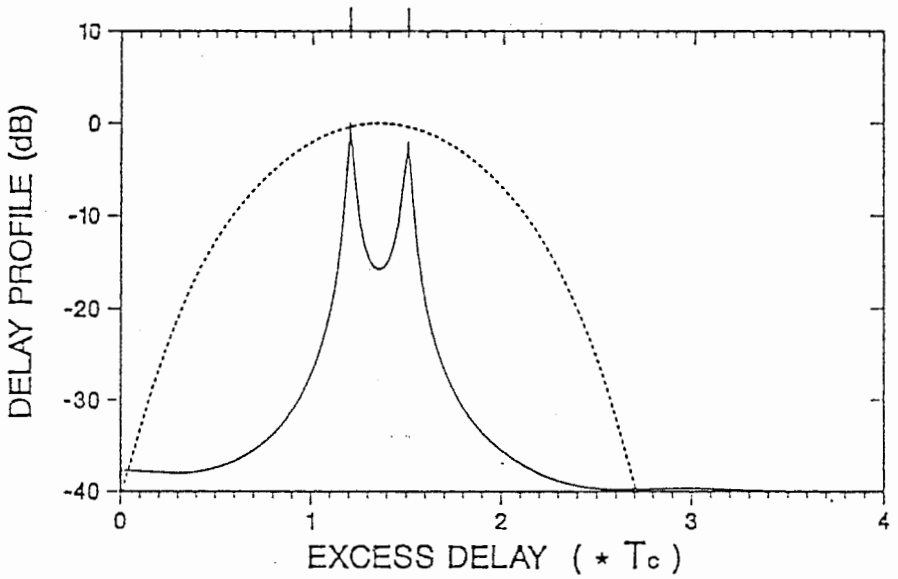

(b) Delay difference 0.3 T_c ($T_1 = 1.2T_c$, $T_2 = 1.5T_c$).

Figure VI.5: Same as Fig. VI.3 except that signal-to-noise ratios are 40 dB.

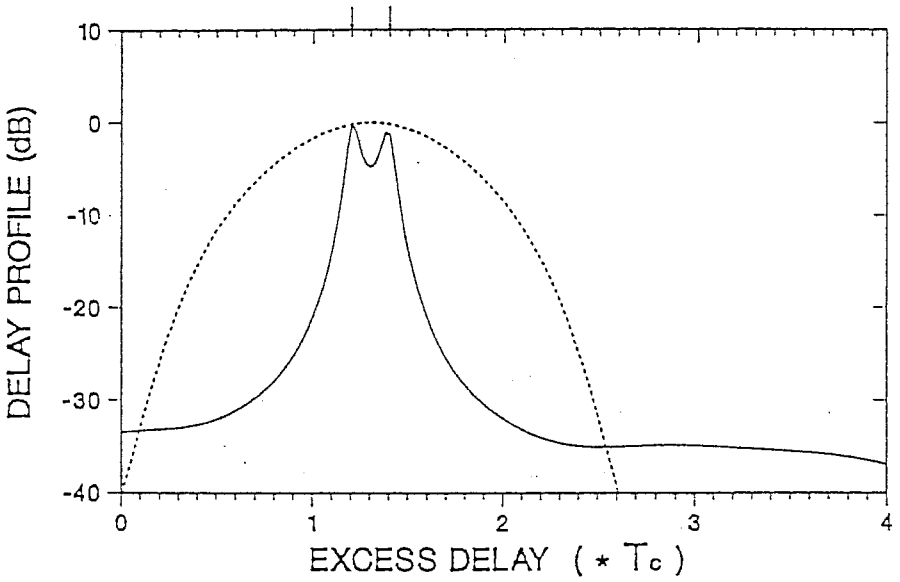

(c) Delay difference 0.2 T_c ($T_1 = 1.2T_c$, $T_2 = 1.4T_c$).

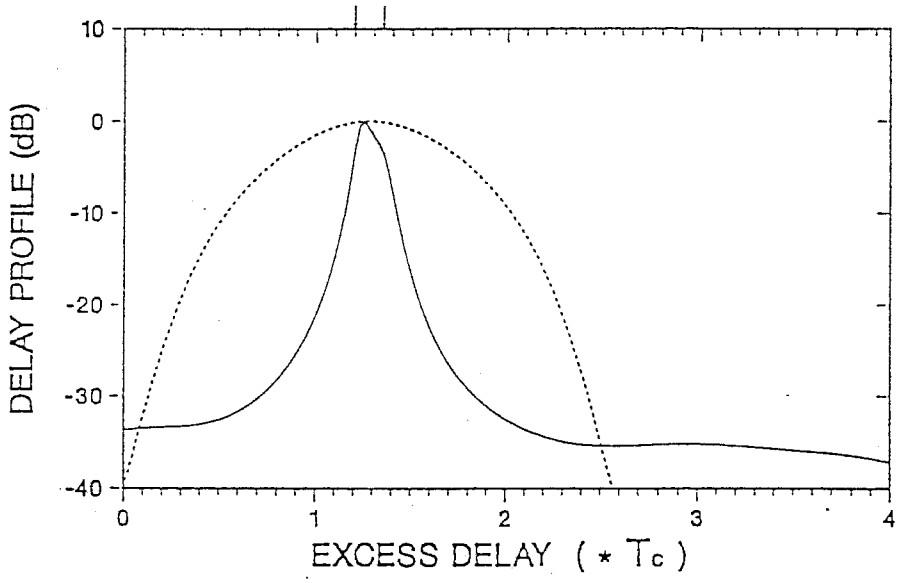

(d) Delay difference 0.15 T_c ($T_1 = 1.2T_c$, $T_2 = 1.35T_c$).

Figure VI.5: Contd.

VI.3. Effects of Band-limitation

The effects of band-limitation in transmitter and receiver upon the performance of the SPM were examined by changing the bandwidth B for the Gaussian filter model given by (IV.2) under the same condition as the case shown in Fig. VI.5(c). Figs. VI.6(a) and (b) show the results obtained for band-limitations of $BT_c = 0.44$ ($\sigma = 0.3\ T_c$) and $BT_c = 0.33$ ($\sigma = 0.4\ T_c$), respectively. By comparing Figs. VI.6(a) and VI.6(b) with Fig. VI.4(c), it is found, as a matter of course, that the wider the bandwidth is, the higher the delay-time resolution is. In the case of $BT_c = 0.33$ shown in Fig. 10, the band limitation is too strict for the SPM to resolve the two paths with a delay-time difference of $0.2\ T_c$.

As a wide-band extreme, Fig. VI.7 shows the result for a fictitious case of a transmitter and receiver without band-limitation. Since the delay time difference is equal to the sampling interval $\Delta\tau = 0.2\ T_c$ in this case, the solution of the SPM is indefinite as described in Section IV, and the delay times cannot be estimated from the resultant delay profile.

Fig. VI.8 shows the effect of mismatching between the actual impulse response of the measurement system and that assumed in the SPM algorithm. In this simulation, multipath transmission channel consisting of two paths with equal amplitudes and equal arrival phases was assumed, and the delay difference of the two paths was assumed to be $0.3T_c$. In this simulation, the data were assumed to be obtained by the measurement system whose overall impulse response $h_{TR}(t)$ was represented by a Gaussian filter with $BT_c = 0.7$. The curves in Fig. VI.8 illustrate the delay profiles estimated by the SPM assuming different bandwidths for the measurement system. Although the error in delay-time estimation increases as the difference between the actual and assumed bandwidths increases, the increase in error is not particularly significant when the bandwidth assumed in the estimation is wider than the actual bandwidth, as far as the delay-time estimation is

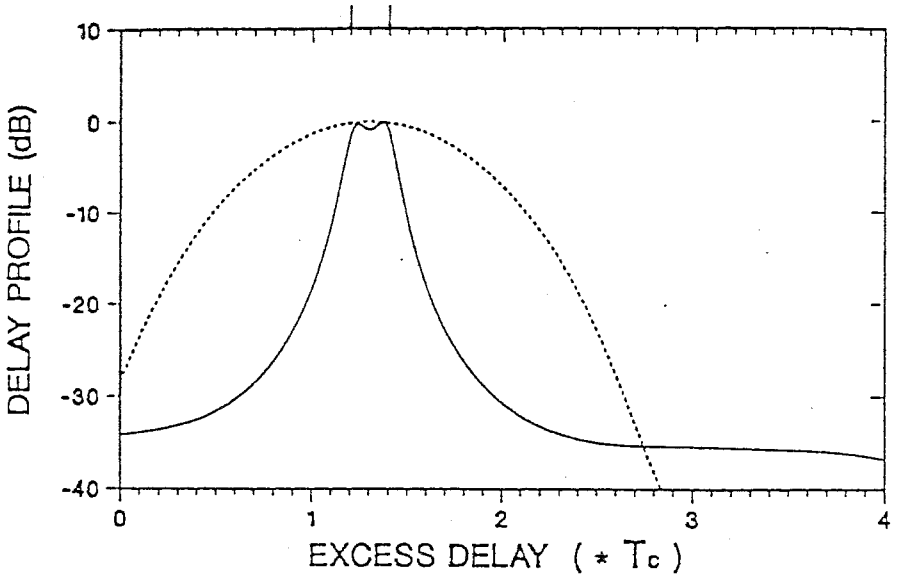

(a) $BT_c = 0.44$ ($\sigma = 0.3\ T_c$).

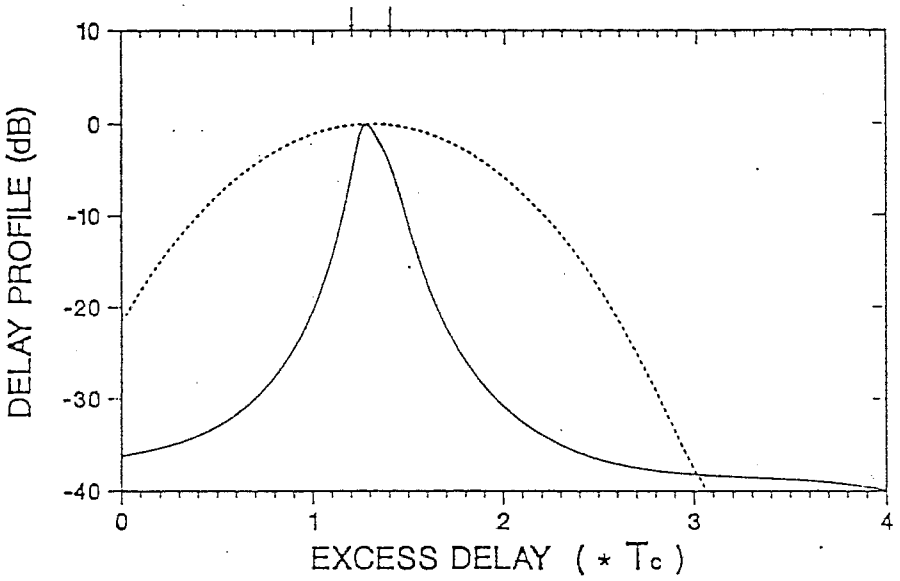

(b) $BT_c = 0.33$ ($\sigma = 0.4\ T_c$).

Figure VI.6. Same as Fig. VI.5(c) except the band-limitation of (a) $BT_c = 0.44$ ($\sigma = 0.3\ T_c$) and (b) $BT_c = 0.33$ ($\sigma = 0.4\ T_c$).

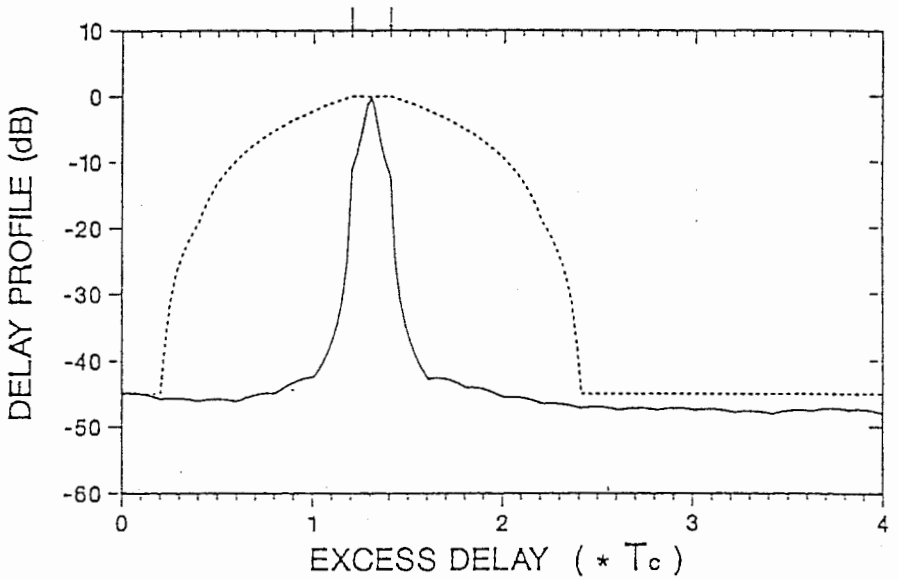

Figure VI.7. Same as Fig. VI.5(c) except that the measurement system is assumed to be band-unlimited.

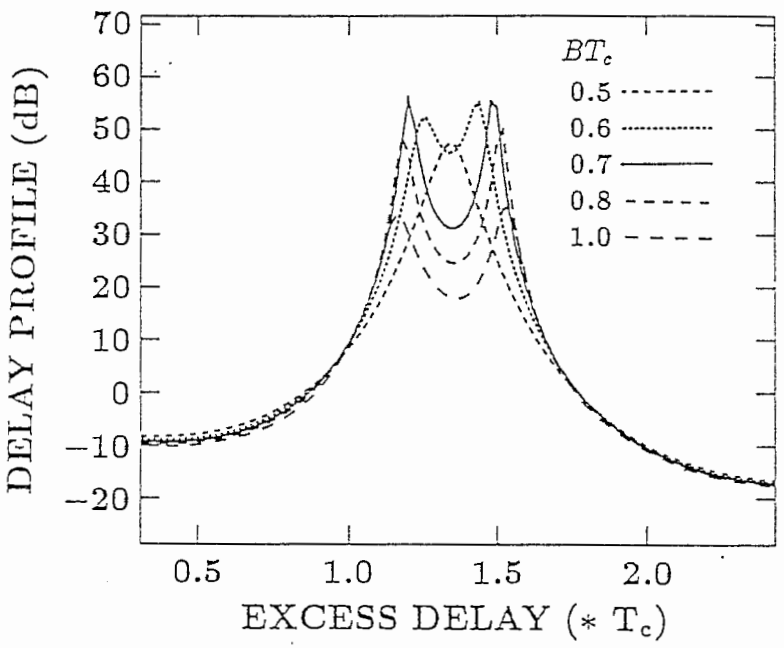

Figure VI.8. Results of superresolution estimation for two-path transmission channel with a delay difference of 0.3 T_c when the bandwidth BT_c of the measurement system assumed in the estimation differs from the actual one $BT_c = 0.7$.

concerned. On the other hand, when the assumed bandwidth is narrower than the actual bandwidth, the delay time resolution deteriorates significantly as the mismatching of the bandwidth increases. This suggests that the bandwidth assumed in the SPM algorithm should not be underestimated.

VII. Experiments

The performance of the SPM has been experimentally verified by applying it to coaxial-cable delay measurements and indoor propagation experiments. The experiments have been carried out with a multipath delay-profile measurement system which had originally been designed to measure complex-valued delay profiles by the conventional PN correlation method.

VII.1. Experimental System

Fig. VII.1 shows the block diagram of the multipath delay-profile measurement system used in the experiments. This experimental system has a capability of measuring delay profiles at 240 MHz, 910 MHz, and 2.3 GHz band. The basic configuration of the system is the same as those used in the conventional PN correlation method [1] except that the additional function of sweeping the carrier frequencies stepwise around the carrier center frequencies enables us to obtain the frequency-averaged correlation matrix as given by (III.5). The pseudonoise (PN) generators at the transmitter and the receiver generate identical 10-stage m-sequences. At the transmitter, the carrier is biphase modulated by this m-sequence at a chip rate of 30 Mchips/s. At the receiver, the received signal is correlated with the identical m-sequence of a slightly lower chip rate, which enables us to obtain delay profiles by the "sliding correlation" technique [1]. The delay-time resolution

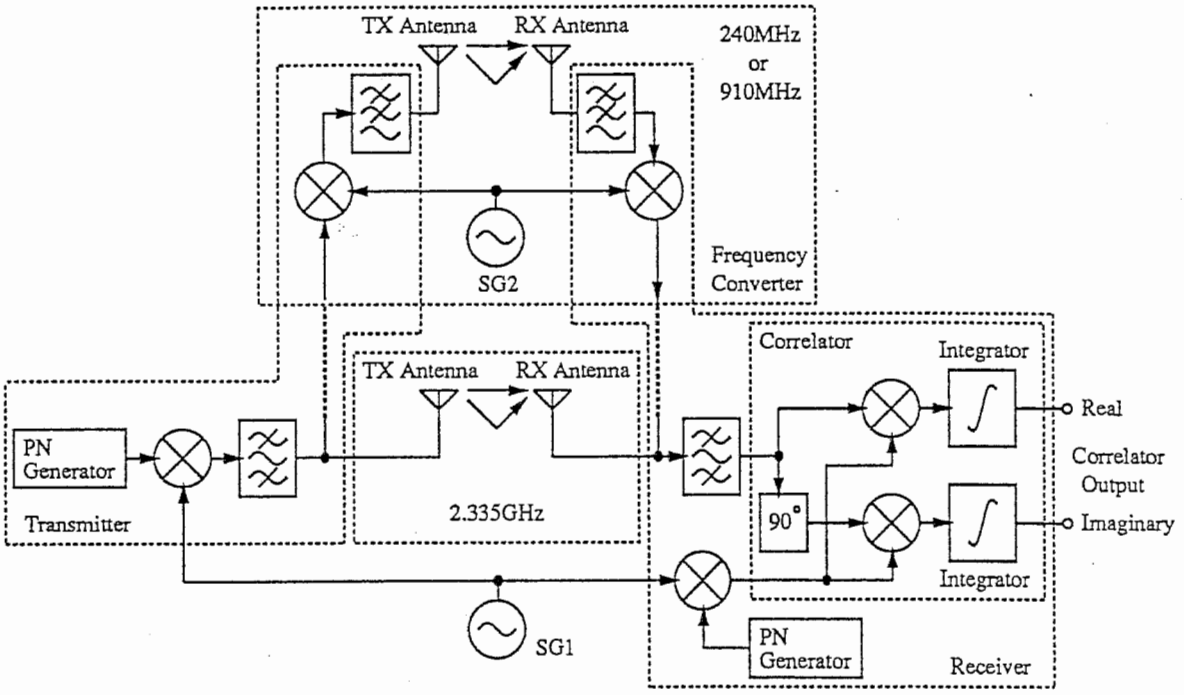

Figure VII.1. Block diagram of the delay-profile measurement system used in experiments

of the conventional PN method is about 33 ns which corresponds to a spatial resolution of about 10 m. Details of the delay-profile measurement system are described elsewhere [18][15].

Since the autocorrelation function used in the SPM delay estimation should be the one which takes the effects of band-limitation into account as described in Section IV, we measured it beforehand by directly connecting the transmitter and the receiver. Since the measured autocorrelation function was found to be approximated by the Gaussian-filtered autocorrelation function given by (IV.1) for a Gaussian filter with $BT_c = 0.7$ ($\sigma = 0.19\ T_c$). We therefore use this approximated autocorrelation function in the following analyses of the experimental results.

VII.2. Resolution of Two Paths

Delay-time resolution of the SPM was experimentally verified for two-path transmission channels. In this experiment, the two-path transmission channel was simulated by connecting a pair of calibrated coaxial delay lines of different lengths in parallel between the transmitter and the receiver. Figs. VII.2(a), (b) and (c) show the results for the 2.3 GHz band by comparing the delay profiles estimated by the SPM (solid curves) with those measured by the conventional PN correlation method at the carrier center frequency $\omega_0 = 2.335$ GHz (dotted curves). The delay profile data vectors were obtained at 5 equispaced frequencies over an interval of $[\omega_0 - 4.19 \times T_c^{-1},\ \omega_0 + 4.19 \times T_c^{-1}]$ and the sampling interval of the delay-profile data was 0.2 T_c as in Simulation II. Figs. VII.2(a), VII.2(b), and VII.2(c) show the results for electric path-length differences of 5.6 m (0.56 T_c), 3.4 m (0.34 T_c), and 1.7 m (0.17 T_c), respectively. Although two paths were not identified in the delay profiles obtained by the conventional PN correlation method shown by dotted curves, two peaks were resolved in the delay profiles estimated by the SPM shown by solid

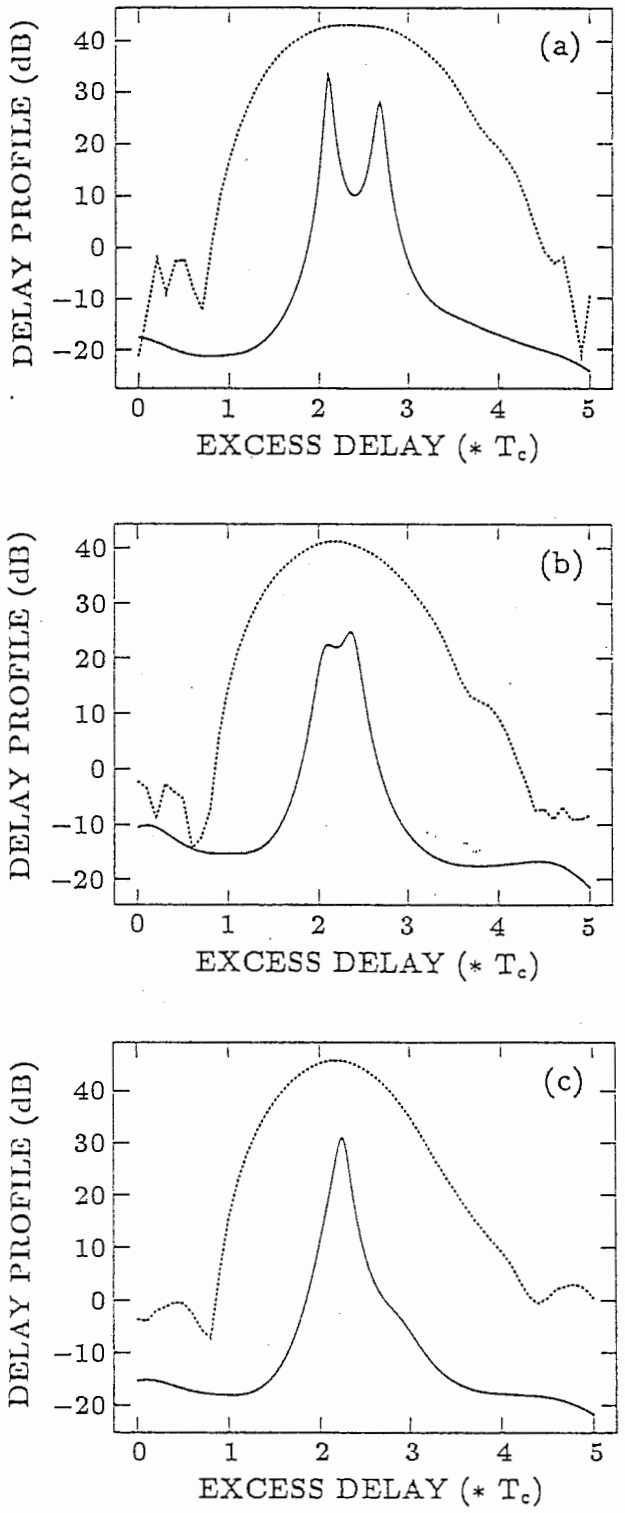

Figure VII.2. Delay profiles of the two-path coaxial delay lines estimated by the SPM (solid curves) and the conventional PN correlation method at 2.335 GHz (dotted curves) for delay differences of (a) 0.56 T_c, (b) 0.23 T_c, and (c) 0.17 T_c.

curves for delay differences above 0.2 GHz. For Figs. VII.2(a) and VII.2(b), delay-time differences estimated from the peak positions of the solid curves were 0.56 T_c and 0.34 T_c which were in excellent agreement with actual delay-time differences.

Similar results were obtained both for 240 and 910 MHz bands. From the results of this experiment and Simulation II, it can be concluded that the resolving power of delay-time difference of the SPM is about 0.2 – 0.3 T_c which corresponds to a difference in path lengths of 2 –3 m when the chip rate of the PN sequence is 30 Mchips/s.

VII.3. Indoor Propagation Experiment

The SPM was applied to the results of the indoor propagation experiments. The multipath-propagation delay profiles were measured in an office room within a building by using the experimental system described in Section VII.1. Fig. VII.3 illustrates the

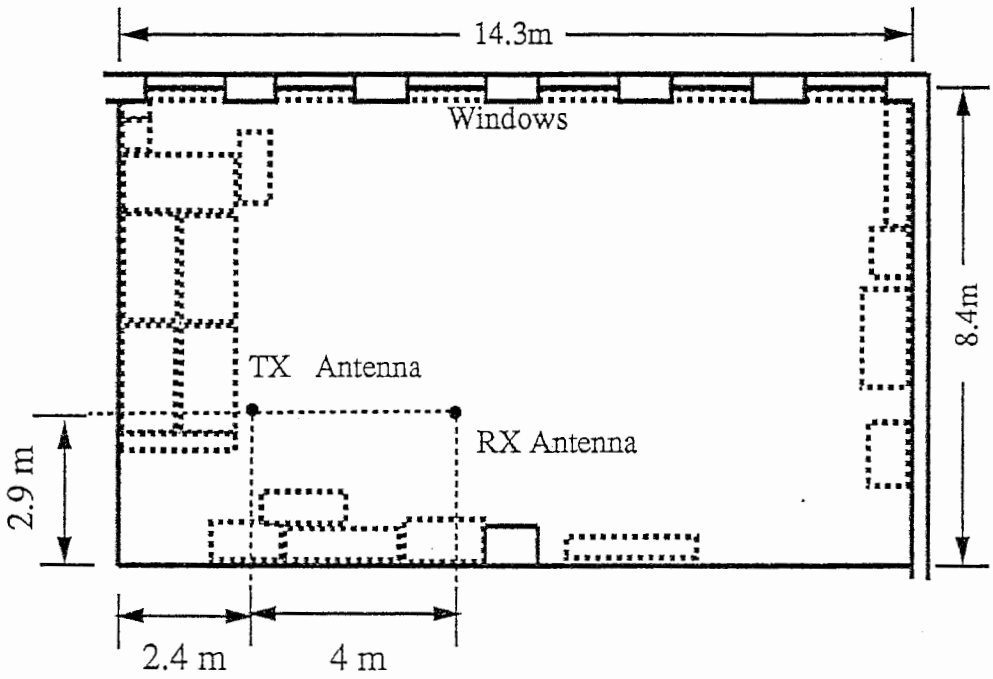

Figure VII.3. Plan of the room used in the indoor experiment. Dotted squares indicate office fixtures.

experimental arrangement of the transmitting and receiving antennas in the room. The height of the ceiling was 2.7 m. Vertically polarized dipole antennas were used for transmitting and receiving antennas. The height of the transmitting and receiving antennas were 2.1 m and 1.2 m, respectively. The delay profile data vectors were obtained at 11 equispaced frequencies over an angular-frequency interval of $[\omega_0 - 4.19 \times T_c^{-1},\ \omega_0 + 4.19 \times T_c^{-1}]$ and the sampling interval of the delay-profile data was 0.2 T_c

Figs. VII.4(a), VII.4(b), and VII.4(c) show the delay profiles measured in the 240 MHz, 910 MHz, and 2.3 GHz bands, respectively. In these Figures. the delay profiles measured by the conventional PN correlation method at the carrier center frequencies and the results of SPM are shown by dotted and solid curves, respectively.

In these Figures, it is found that six or seven peaks are resolved in the results of the SPM (solid curves) while only three or four peaks can be identified in the delay profiles measured by the conventional PN correlation method (dotted curves). Periodic fine structures are found in the results of the SPM, and the positions of peaks relative to the first peak, though some peaks are missing, are in good agreement in these three Figures independent of the frequency band used in the experiments. These periodical fine structures suggest the existence of multiple reflections in which waves traveling back and forth between facing walls. From the geometrical arrangement of the transmitter and receiver, these periodical fine structures with a fundamental period of about 1.t T_c (= 50 ns) can be explained by the multiple reflections between the left-side and right-side walls in Fig. VII.3 [19].

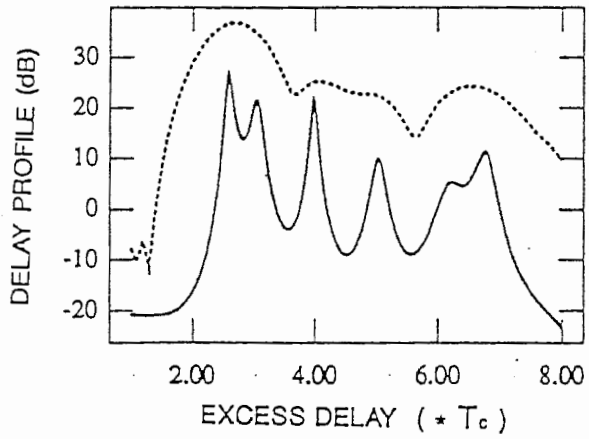

(a) 240 MHz

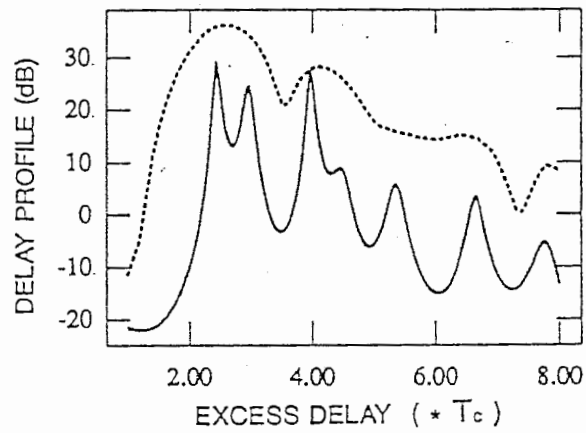

(b) 910 MHz

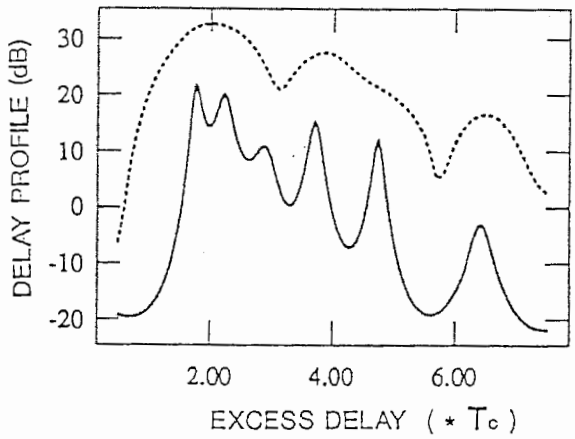

(c) 2.3 GHz

Figure VII.4. Indoor delay profiles measured using the conventional PN correlation method (dotted curve) and the results of its superresolution estimation using the SPM (solid curve).

VIII. Conclusion

In this paper, we have proposed the superresolution PN correlation method (SPM) to improve the time resolution of delay profiles measured by the conventional PN correlation method. The SPM is based on eigen-decomposition of the data correlation matrix as in the MUSIC algorithm. Superior delay-time resolution of the SPM has been verified by computer simulations and experiments with coaxial delay lines. This method has enabled us to resolve the delay-time differences as small as about 0.2 T_c, which correspond to a spatial resolution of about 2 m for free space when a PN sequence of 30 Mchips/s is employed.

The applicability of the SPM to the analyses of the indoor multipath propagation has been demonstrated by applying this method to delay profiles obtained at 240 MHz, 910 MHz, and 2.3 GHz within an office room. Detailed analysis of the results of the indoor propagation experiments and a modeling of the propagation within the room will be described elsewhere [15][19].

Appendix A

This Appendix introduces a computationally stable and efficient method to solve the generalized eigenvalue problem given by

$$R\,e = \lambda R_0\,e \tag{A.1}$$

where R is a positive-definite Hermitian matrix and R_0 is a positive-definite symmetric matrix [20].

Although this eigenvalue problem can be solved by transforming it into an equivalent simple eigenvalue problem

$$R_0^{-1}\,R\,e = \lambda e, \tag{A.2}$$

it is well known that the solution to this problem is unstable when some of the eigenvalues of R are very small.

Stable solution can be obtained by using the Cholesky factorization of the symmetric matrix. The Cholesky factorization of the real symmetric matrix R_0 with a upper triangular matrix U is given by

$$R_0 = U^t U. \tag{A.3}$$

By using this Cholesky factorization, the generalized eigenvalue problem given by (A.1) can be written as

$$\tilde{R}\,\tilde{e} = \lambda \tilde{e}, \tag{A.4}$$

where $\tilde{R}$ is a positive-definite Hermitian matrix given by

$$\tilde{R} = U^{-1^t} R U^{-1}, \tag{A.5}$$

and

$$\tilde{e} = U\,e. \tag{A.6}$$

The solution of the eigenvalue equation given by (A.4) is much more stable than that of (A.1), and the eigenvectors of (A.1) is obtained by

$$e = U^{-1}\,\tilde{e}. \tag{A.7}$$

By using the Cholesky decomposition of the matrix $\boldsymbol{R}_0$, the numerator of (III.7) can be efficiently calculated by using the following equation:

$$\begin{aligned} \boldsymbol{r}(\tau)^t \boldsymbol{R}_0^{-1} \boldsymbol{r}(\tau) &= \boldsymbol{r}(\tau)^t (U^t U)^{-1} \boldsymbol{r}(\tau) \\ &= |(U^t)^{-1} \boldsymbol{r}(\tau)|^2. \end{aligned} \tag{A.8}$$

Appendix B

Let the delay profile $z(\tau)$ be sampled at equispaced intervals $\Delta\tau$ such that $\tau_n = n\Delta\tau$ and $T_c = \eta\Delta\tau$ where η is an integer. Suppose that the delay time of the ith path, T_i, is in a time interval given by $N\Delta\tau \leq T_i \leq (N+1)\Delta\tau$. Then, $T_i = N\Delta\tau + \zeta_i$ where $0 \leq \zeta_i \leq \Delta\tau$. In this case, it can be readily shown that the mode vector for the ith path is given by

$$\boldsymbol{r}(T_i) = \boldsymbol{r}(N\Delta\tau) + \zeta_i \Delta\boldsymbol{r}, \tag{B.9}$$

where the lth component of $\Delta\boldsymbol{r}$ is given by

$$\Delta r_l = \begin{cases} -\dfrac{1+\xi}{T_c} & \text{for} \quad N-\eta+1 \leq l \leq N, \\[2ex] \dfrac{1+\xi}{T_c} & \text{for} \quad N+1 \leq l \leq N+\eta, \\[2ex] 0 & \text{otherwise.} \end{cases} \tag{B.10}$$

In (B.10), ξ is a constant determined by the length 2^m of the m-sequence as $\xi = 2^{-m}$ where m is the number of the stages of the shift register used to generate the m-sequence. It should be noted that $r(N\Delta\tau)$ and Δr are independent of ζ_i. This is due to the fact that the autocorrelation function of the m-sequence has a rectilinear waveform as shown in Fig. II.1.

In order to examine the delay-time resolution, consider a multipath environment ($M = 2$) with only two paths whose delay times T_1 and T_2 are assumed to be within a sampling interval $N\Delta\tau \leq T_1, T_2 \leq (N+1)\Delta\tau$. If we ignore the noise term in (III.1) for simplicity, the data vector z is given by

$$z = h_1' r(T_1) + h_2' r(T_2) \tag{B.11}$$

$$= (h_1' + h_2') r(N\Delta\tau) + (h_1'\zeta_1 + h_2'\zeta_2)\Delta r \tag{B.12}$$

where $h_i' = h_i e^{-j\omega T_i}$ $(i = 1, 2)$. It can readily be shown that the set of variables $\{h_1', \zeta_1, h_2', \zeta_2\}$ which satisfies (B.12) cannot be uniquely determined for given data vector z. This implies that the delay times of two or more paths arriving within a sampling interval $\Delta\tau$ cannot be determined uniquely when the measurement system is band-unlimited. This indefiniteness is a direct consequence of the rectilinear wave form of the triangular autocorrelation function and can be evaded when the band-limitation of the system is taken into account.

Acknowledgment

The authors are greatly indebted to Eiichi Ogawa (ATR), Tokio Taga (NTT), and Hiroyuki Imahori (Kyocera) for installing the delay-profile measurement system. We would like to thank Keigo Iizuka (Univ. of Toronto) and Wataru Matsui (ATR) for their helpful suggestions and discussions about the PN correlation method and the modeling of indoor propagation. We wish to express sincere thanks to Yoji Furuhama, Masami Akaike and other staff of ATR Optical and Radio Communications Research Laboratories for their continual encouragement and discussions throughout this research.

Bibliography

[1] D. C. Cox, "Delay Doppler characteristics of multipath propagation at 910 MHz in a suburban mobile radio environment," *IEEE Trans. Antennas Propagat.*, vol. **AP-20**, no. 5, pp. 625 – 635, Sept. 1972.

[2] D. Molkdar, "Review on radio propagation into and within buildings," *IEE Proc.-H,* vol. **138**, no. 1, pp. 61 – 73, Jan. 1991.

[3] A. M. Saleh and R. A. Valenzuela, "A statistical model for indoor multipath propagation," *IEEE J. Selec. Areas Commun.,* vol. **5**, no. 2, 128 – 137, Feb. 1987.

[4] T. S. Rappaport, "Characterization of UHF multipath radio channels in factory buildings," *IEEE Trans. Antennas Propagat.,* vol. **AP-37**, no. 8, pp. 1058 – 1069, Aug. 1989.

[5] D. A. Hawbaker and T. S. Rappaport, "Indoor wideband radiowave propagation measurements at 1.3 GHz and 4.0 GHz," *Electron. Lett.,* vol. **26**, no. 21, pp. 1800 –1802, Sept. 1990.

[6] S. Obayashi and T. Maeda, "Effects of base station antenna height on indoor radio propagation delay characteristics," *1990 Spring National Convention Record, IEICE, Japan*, SB-1-2, 1990.

[7] S. Obayashi and T. Maeda, "Time variation of the magnitude and phase of multipath delay in practical indoor radio channels," in *Proc. 7th Int. Conf. on Antennas and*

Propagation, York, UK, Apr. 1991.

[8] D. M. J. Devasirvatham, "Time delay spread and signal level measurements of 850 MHz radio waves in building environments," *IEEE Trans. Antennas Propagat.,* vol. **AP-34**, no. 11, pp 1300 – 1305, Nov. 1986.

[9] R. J. C. Bultitude, S. A. Mohmoud, and W. A. Sullivan, "Comparison of indoor radio propagation characteristics at 910 MHz and 1.75 GHz," *IEEE J. Selec. Areas Commun.,* vol. **7**, no. 1, pp. 20 – 30, Jan. 1989.

[10] M. Sako, T. Takeuchi, Y. Sueyoshi, S. Sonoda, and S. Yoshida, "Results of indoor delay profile measurement at 1.5 GHz," *IECE Tech. Rep.,* A·P 89-46, 1989.

[11] R. O. Schmidt, "Multiple emitter location and signal parameter estimation," *IEEE Trans. Antennas Propagat.,* vol. **AP-34**, no. 3, pp. 276 – 280, Mar. 1986.

[12] H. Yamada, Y. Ogawa, M. Ohmiya, and K. Itoh, "Fundamental study on antenna measurements using a superresolution technique," *IECE Tech. Rep.,* A·P 90-47, 1990.

[13] N. Kikuma, M. Anzai, M. Ogawa, K. Yamada, and N. Inagaki, "Estimation of direction of arrival and delay profile of multipath waves by MUSIC algorithm for indoor radio communications," *Trans. IEICE,* **J73-BII**, no. 11, pp. 786 –795, 1990.

[14] T. Manabe and H. Takai, "Superresolution of delay profiles measured by pulse-compression method," *IEICE Tech. Rep.,* A·P 90–108, Jan. 1991. [Submitted to *IEEE Trans. Antennas Propagat.,*]

[15] H. Takai and T. Manabe, "An analysis of indoor propagation using delay profiles measured by superresolution pulse-compression method," *IEICE Tech. Rep.,* A·P 90–109, Jan. 1991.[Submitted to *IEEE Trans. Veh. Technol.,*]

[16] F. Haber and M. Zoltowski, "Spatial spectrum estimation in a coherent signal environment using an array in motion," *IEEE Trans. Antennas Propagat.,* **AP-34**, no.

3, Mar. 1986.

[17] E. R. Ferrara and T. M. Parks, "Direction finding with an array of antennas having diverse polarizations," *IEEE Trans. Antennas Propagat.*, **AP-31**, no. 2, pp 231 – 236, Mar. 1983.

[18] H. Imahori, "Studies on multipath propagation characteristics and equalization system," *ATR Technical Report,* TR–O–0034, Sep. 1990.

[19] H. Takai and T. Manabe, "An indoor propagation analysis using delay profiles measured by the superresolution pulse-compression method," 1991 North American Radio Science Meeting and International IEEE/AP-S Symposium, London, Ontario, Canada, June 1991.

[20] Mathematical Society of Japan, "Suugaku-jiten," 3rd ed., p 350, Iwanami-shoten, Tokyo, Japan, 1985.